ScientificScholar®
Knowledge is power
Publisher of Scientific Journals

www.clinicalimagingscience.org

Journal of Clinical Imaging Science

Review Article *Genitourinary and Gynecologic Imaging*

Computed tomography and magnetic resonance imaging characteristics of renal cell carcinoma: Differences between subtypes and clinical evaluation

Ahmet Baytok[1], Gökhan Ecer[2], Mehmet Balasar[3], Mustafa Koplay[4]

Departments of [1]Radiology and [2]Urology, Karapınar State Hospital, [3]Department of Urology, Necmettin Erbakan University, School of Medicine, [4]Department of Radiology, Selcuk University, School of Medicine, Medical Faculty, Konya, Turkey.

***Corresponding author:**
Ahmet Baytok,
Departments of Radiology
Karapınar State Hospital,
Konya, Turkey.

drahmetbaytok@gmail.com

Received: 24 November 2024
Accepted: 03 January 2025
Published: 25 February 2025

DOI
10.25259/JCIS_160_2024

Quick Response Code:

ABSTRACT

This review discusses the evaluation of renal cell carcinoma (RCC) subtypes using computed tomography (CT) and magnetic resonance imaging (MRI). RCC is a malignancy with different histopathological subtypes, constituting approximately 90% of adult kidney tumors. It has been reported that these subtypes show significant differences in terms of clinical behavior, treatment response, and prognosis. In the study, CT and MRI findings of subtypes such as clear cell RCC (ccRCC), papillary RCC (pRCC), chromophobe RCC (chRCC), medullary RCC (mRCC), collecting duct RCC (cdRCC), and multiloculated cystic RCC (mcRCC) were compared. It was stated that CT is the first-choice imaging method in the staging and surgical planning of RCC and provides detailed information about the tumor size, vascularity, and metastatic spread. On the other hand, it has been emphasized that MRI allows better characterization of RCC subtypes with its soft-tissue resolution and contrast agent usage advantage. The study draws attention to the different imaging features of each subtype and details the role of these findings in the clinical decision-making process. It has been stated that ccRCC exhibits intense contrast enhancement and rapid washout pattern in the corticomedullary phase on CT and appears hyperintense on T2A and hypointense on T1 weighted imaging (T1A) on MRI. It has been stated that pRCC has hypovascular features, has lower contrast enhancement, and has homogeneous borders. It has been stated that chRCC has a less vascular structure and exhibits moderate contrast enhancement in the corticomedullary phase. It has been reported that mRCC has invasive features and is usually diagnosed at an advanced stage while cdRCC has a very aggressive clinical course. It has been stated that mcRCC contains distinct cystic areas between the septa, has a well-circumscribed structure, and generally has a low malignancy potential. As a result, it has been stated that detailed evaluation of CT and MRI findings of RCC subtypes plays a critical role in the diagnosis, treatment, and prognosis of these subtypes. It has been emphasized that the findings presented in this study will contribute to the development of more targeted treatment approaches in RCC management.

Keywords: Renal cell carcinoma, Computed tomography imaging, Magnetic resonance imaging, Papillary renal cell carcinoma, Clear cell renal cell carcinoma

INTRODUCTION

Renal cell carcinoma (RCC) is a malignancy that accounts for approximately 90% of adult kidney tumors and is generally known as a disease with a high rate of metastatic diagnosis. One of the most important features of RCC is that it is divided into a wide variety of histopathological subtypes. These subtypes show significant differences in terms of clinical behavior, treatment response, and prognosis. Clear cell RCC (ccRCC) is the most common subtype and accounts for

70–80% of all RCC cases. Papillary RCC (pRCC) is seen in approximately 10–15%, while chromophobe RCC (chRCC) is less common and is diagnosed in 5%. Less common RCC subtypes include medullary RCC (mRCC), collecting duct RCC (cdRCC), and multiloculated cystic RCC (mcRCC), but these types, although rare, can have quite aggressive clinical courses.[1-3]

Radiological methods such as computed tomography (CT) and magnetic resonance imaging (MRI) play a critical role in the diagnosis of RCC subtypes. CT is one of the first-choice imaging methods for staging and surgical planning of RCC and provides detailed information about the size, vascularity, and metastatic spread of tumor. On the other hand, MRI offers significant advantages in terms of contrast agent use and allows better characterization of RCC subtypes, especially thanks to its soft-tissue resolution. Imaging findings can help determine the histopathological subtype of the tumor and play an important role in the clinical decision process in terms of predicting the patient's prognosis.[4,5]

This review will address the CT and MRI imaging characteristics of RCC subtypes, with a detailed assessment of the characteristic findings of each subtype. The imaging features of RCC types will be highlighted, and the clinical and prognostic significance of these findings will be examined.

MATERIAL AND METHODS

In this review, studies conducted in 15 years to examine the CT and MRI features of RCC subtypes were evaluated. The study was conducted with a comprehensive literature review aiming to access up-to-date and reliable information. PubMed and Google Scholar databases were used to scan the studies included in the research.

Screening method

During the literature review, keywords targeting various subtypes of RCC and their CT and MRI findings were used. These keywords are RCC, ccRCC, pRCC, chRCC, mRCC, Bellini duct carcinoma, multilocular cystic RCC, CT, MRI, imaging features, and tumor subtype characterization in the past 15 years.

Inclusion and exclusion criteria

Included studies

Original research articles examining the CT and MRI features of RCC subtypes were included in the screening process. These studies included detailed reviews of histopathological and imaging findings of different RCC subtypes. The publication dates of the studies were limited to a 15-year period (2009–2024).

Excluded studies

Small case series, studies with limited sample sizes, systematic reviews, and studies that did not provide sufficient histopathological information on RCC subtypes or focused only on invasive methods such as biopsy were excluded from the screening [Figure 1].

CT AND MRI TECHNIQUES IN FOCUS: IMAGING CHARACTERISTICS ACROSS RCC SUBTYPES

CT and RCC subtypes

CT is one of the basic imaging methods in the diagnosis and staging of RCC and shows different contrast enhancement patterns according to tumor subtype and vascularity. Routine dynamic CT examination consists of pre-contrast and post-contrast multiphasic images. In pre-contrast examination, fat, calcification, and hemorrhage areas in the lesion content are detected and density measurement is also performed to contribute to lesion characterization.[6] The post-contrast series are known as the corticomedullary phase (after 20–45 s), nephrogenic phase (after 60–90 s), and excretory phase (after >5 min). In the corticomedullary phase, the renal cortex shows peak enhancement and becomes more prominent compared to the hypovascular medulla; thus, the vascularization of tumors localized in the cortex, their relationship with neighboring vascular structures, and hypervascular metastases, if any, can be detected. However, the nephrogenic phase, in which the parenchyma is uniformly enhanced, plays an important role in the detection of small hypovascular masses that may be overlooked in the corticomedullary phase. In the excretory phase, the relationship of the lesions with the collecting ducts and ureter is determined.

The choice of contrast agents is also of great importance in the detection and diagnosis of ccRCC. Various contrast agents allow for better visualization of the vascular structure of the tumor and allow for clearer differentiation of lesions. Commonly used contrast agents such as iopamidol and iohexol allow the characteristic vascular structure of ccRCC to be visualized on CT.[7] Especially in large lesions, the uniform distribution of contrast agents helps to better detect the size and borders of tumor.[8]

ccRCC

Known as the most common type of RCC and originating from the proximal tubule, these tumors are characterized by intense contrast enhancement in the corticomedullary phase and rapid wash-out in the nephrogenic phase. The tumor usually has irregular borders and is markedly hypervascular.[9] In particular, patients with localized RCC

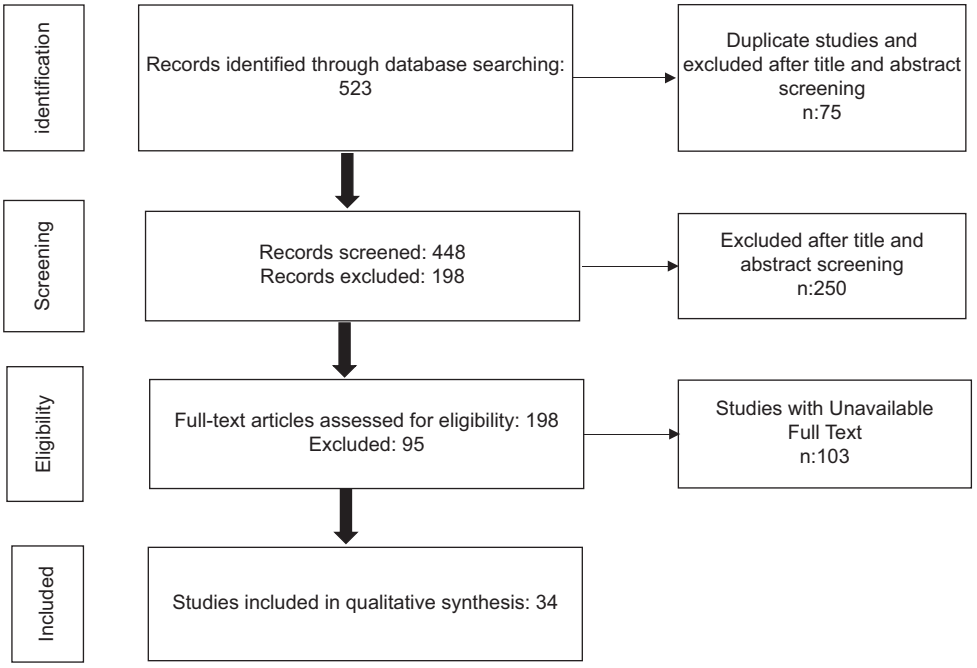

Figure 1: PRISMA flow diagram.

lesions without surrounding invasion or distant metastasis had a significantly higher 5-year survival rate (91.7%), highlighting the critical importance of early diagnosis in improving patient survival[10] [Figure 2].

CcRCC usually presents as heterogeneous iso-hypodense lesions compared to normal renal parenchyma on CT. The characteristic feature of ccRCC on IV contrast-enhanced CT is rapid wash-in and wash-out. The tumor shows rapid and intense contrast enhancement in the corticomedullary phase, while in the nephrogenic phase, the density of the lesion, which shows rapid contrast washout, decreases rapidly and becomes lower than the surrounding renal parenchyma. In addition, more heterogeneous enhancement is seen in ccRCC.[11]

In the study conducted by Wang *et al*., it was reported that CT had 88% sensitivity and 82% specificity in detecting ccRCC.[9] Depending on the level of vascularity, tumors may show homogeneous or heterogeneous enhancement, which helps distinguish ccRCC from other renal tumors.[10] Zhu *et al*. and Gentili *et al.* compared RCC subtypes with imaging findings, emphasizing the importance of contrast patterns in distinguishing ccRCC from oncocytoma (ONC).[12,13]

pRCC

Known as the second most common type of RCC and originating from the proximal tubule, these tumors are prominent with their hypovascular characteristics and exhibit lower contrast enhancement after Intravenous (IV) contrast injection. This tumor, which does not show significant contrast enhancement in the corticomedullary phase on dynamic CT examination, reaches peak enhancement level in the nephrogenic phase. Compared to ccRCC, pRCC usually has more homogeneous and regular borders[14] [Figure 3].

It is known that pRCC shows less contrast enhancement than ccRCC.[15] This difference in contrast enhancement is related to the microvascular density within the tumor. Calcification is more common in pRCC than in ccRCC on non-contrast CT. However, the presence of calcification is not significant in distinguishing these two tumors.[16]

There are two types of pRCC. Type 1 consists of small cells with basophilic cytoplasm and uniform small round nuclei, while type 2 consists of large cells with eosinophilic cytoplasm and large spherical-shaped nuclei.[17] Murugan *et al*.'s (2022) study examined the long-term follow-up results of 199 pRCC cases and revealed that type 1 pRCC has a better prognosis.[16]

The study by Delahunt *et al*. shows that type 1 and type 2 pRCC are morphologically defined for the 1st time. It is emphasized that type 2 pRCC has a larger tumor size and higher nuclear grade. This suggests that type 2 pRCC may follow a more aggressive course and is also invasive on CT imaging.[18] The study by Klatte *et al*. shows that type 1 pRCC tends to show a more limited growth and invasion pattern on CT imaging.[19]

The study by Sukov *et al*. showed that larger tumors and cases with lymphovascular invasion had a more aggressive and widespread appearance on CT. These findings support

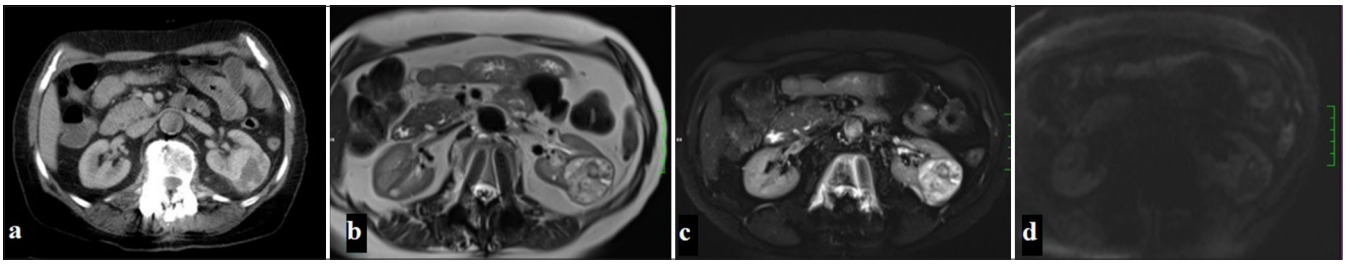

Figure 2: (a) A 65-year-old woman with a mass in the left kidney observed on CT in the portal phase, (b) On MRI, the mass appears heterogeneously hyperintense on T2-weighted and fat-suppressed T2-weighted images,(c) while areas within the mass demonstrate focal diffusion restriction on diffusion-weighted imaging (DWI) (d) and apparent diffusion coefficient (ADC) maps.

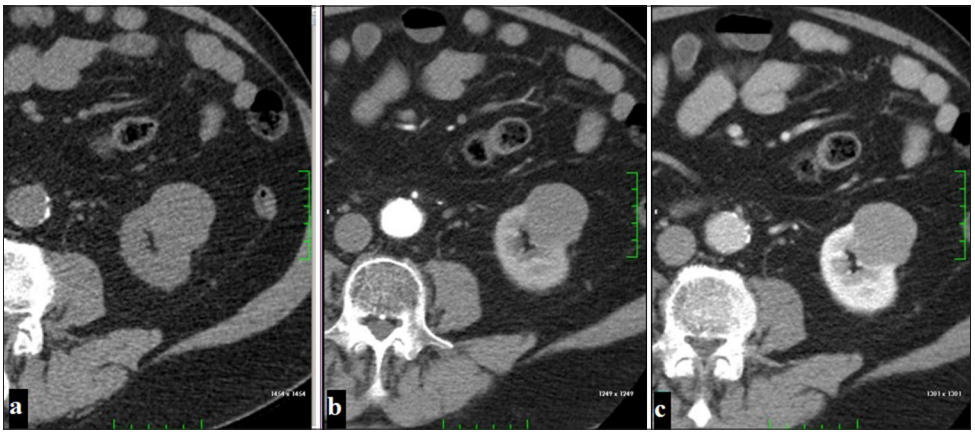

Figure 3: A 54-year-old man with a localized exophytic mass lesion in the left kidney, showing no significant contrast enhancement (a) on the pre-contrast phase, (b) corticomedullary phase, (c) nephrogenic phase images (Papillary renal cell carcinoma).

the general understanding that type 2 pRCC generally has a worse prognosis and is more obvious on imaging.[20]

Type 1 pRCC generally has a better prognosis and a more limited pattern of invasion, which may be associated with less aggressive findings on CT and MRI, while type 2 pRCC may have a more aggressive and invasive course. This information provides important clues on how to interpret imaging findings in the diagnosis and treatment of pRCC.[21]

chRCC

This subtype of RCC, which is the third most common and originates from the collecting duct, shows a homogeneous structure. The tumor, which can show different contrast enhancement patterns in IV contrast-enhanced CT examinations, most often shows moderate contrast enhancement in the corticomedullary phase. While no significant vascularity is observed in dynamic CT images of this type, it tends to have less contrast enhancement than ccRCC[22] [Figure 4].

Studies on chRCC show that these tumors generally have a better prognosis and that imaging findings are typically well-circumscribed, hypodense lesions. Amin *et al*. emphasize

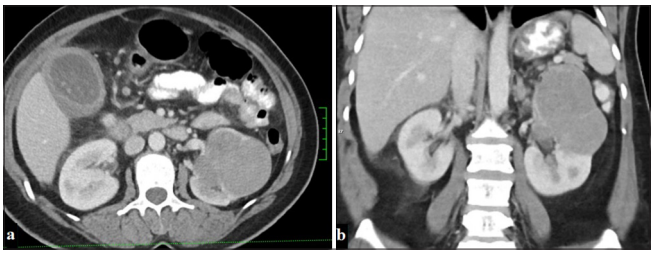

Figure 4: A 53-year-old woman with a mass lesion in the upper pole of the left kidney, displaying macrolobulated contours and minimal contrast enhancement in the portal phase on (a) axial and (b) coronal planes on CT (Chromophobe renal cell carcinoma).

that chRCC has lower metastasis rates than other subtypes, while these tumors have higher long-term survival rates.[23,24] It has also been found that tumor size, small vessel invasion, and necrosis are associated with poor prognosis.[25]

mRCC

It is one of the aggressive types of RCC and has an irregular and invasive appearance on CT. It is usually hypovascular

and does not show significant contrast enhancement in the late phase.[26] The known features are the tendency to involve the right kidney, caliectasis, intratumoral necrosis, and accompanying lymphadenopathy.[27]

In the 2024 study by Lebenthal *et al*., a distinction was made between mRCC with SWI/SNF-related matrix-associated actin-dependent regulator of chromatin subfamily B member 1 (SMARCB1) deficiency and RCCU-MP (RCC, medullary phenotype), the subtype of RCC with a medullary phenotype. The study emphasizes that mRCC often presents with hematuria and usually metastasizes to retroperitoneal lymph nodes.[28]

MRCC is a rare and aggressive tumor that is usually seen in young patients with sickle cell disease, especially in African individuals, and imaging findings provide important clinical clues. Studies emphasize that these tumors are usually diagnosed at an advanced stage and have a heterogeneous structure with no clear borders on imaging.[29]

Lebenthal *et al*. study demonstrates the current management approaches and improved survival with response to treatment. This study examines the differences between mRCC and RCCU-MP (RCC, medullary phenotype) associated with SMARCB1 deficiency and indicates that current imaging techniques are important in better characterizing tumor spread. In addition, retroperitoneal lymph node metastases are frequently observed in these tumors and methods such as CT and MRI play a critical role in the diagnosis of metastases.[28]

Collecting duct RCC (cdRCC)

This rare subtype, which is located in the medullary region and has a very aggressive course, has invasive and irregular borders on CT. As the tumor size increases, it can extend from the medulla to the renal pelvis and cortex, hemorrhage, and necrosis areas and cystic components are also noted within the tumor.[30] A heterogeneous uptake is observed after IV contrast injection.

In the study by Karakiewicz *et al*., it was stated that the prognosis of cdRCC is quite poor and is mostly metastatic at the time of diagnosis. On imaging, it was determined that these tumors usually invade the renal sinus.[31]

In the study by Gupta *et al*., mRCC and cdRCC were compared clinically and histopathologically. The study revealed that although there were some similarities between the two tumor types, mRCC had a worse prognosis.[26] CdRCC has been shown to be medullary, poorly contrasting, and frequently cystic.[32,33]

mcRCC

A multiloculated cystic tumor with a fibrous capsule containing cystic areas of different sizes separated by septa on CT may show different degrees of contrast enhancement in the septa after IV contrast.[34] Calcification can be observed in the walls and septa in approximately 20% of tumors.

McRCC radiologically contains well-defined cystic structures and is a cystic mass separated by septa with minimal or no solid components within the tumor. In CT and MRI, these cystic structures usually have thin, regular septa, and mild contrast enhancement is observed in the septa after contrast injection.[34,35] These tumors are usually located in the renal cortex and contain distinct cystic structures.[34]

In two recent studies, methods such as contrast-enhanced ultrasound (CEUS), contrast-enhanced computed tomography (CECT), and lipid-to-carbohydrate ratio (L/C) ratio provided effective measurements in distinguishing RCC subtypes.[36,37] These studies support the importance of imaging features in the diagnosis of subtypes of RCC [Table 1].

MRI and RCC subtypes

Although CT examination is the most commonly used method in the diagnosis of RCC, MRI examination is an imaging method that has been increasingly used in recent years due to its advantages such as not containing ionizing radiation, high contrast resolution, and functional imaging techniques. Conventional sequences used in MRI consist of T2-weighted imaging (T2WI), chemical shift imaging (CSI, in and out phases), and T1-weighted images (T1WIs) taken before and after IV gadolinium injection (T1WI).[38] The combination of these sequences with dynamic contrast-enhanced examinations and diffusion weight imaging (DWI) is defined as multiparametric MRI. MRI provides the advantage of providing detailed information in terms of soft-tissue resolution of RCC and plays an important role in tumor characterization with signal intensities in different subtypes.

The presence of intratumoral fat plays a critical role in the differential diagnosis of RCC types. While intralesional macroscopic fat is detected by frequency selective fat suppression techniques, microscopic fat can only be detected in gradient echo sequences (in and out phases). The presence of lipid within the tumor shows increased signal in the in phases, while signal loss is noted in the out phases.[39]

ccRCC

The most common type of all RCC and ccRCC is 95% sporadic. However, it can also be encountered rarely with familial and Von Hippel–Lindau disease. The vast majority of cases are associated with 3p deletion.[40] It is more symptomatic than other types and is often encountered as advanced stage and metastatic disease.[23] On MRI, it appears iso-hypointense with

Table 1: Summary of RCC imaging characteristics and study details on CT.

Study	Study design	Number of patients	Mean age (years)	Tumor type	Tumor size (cm)	Vascularity	Main finding
Klatte *et al.*, (2009)[19]	Retrospective	158	61,9	pRCC (Type 1/2)	4,9/6,6	Vascular invasion: 35% (Type 2) versus 10% (Type 1).	Type 1 pRCC was generally found to be less aggressive and trisomy 7 and 17 gains were more common.
Sukov *et al.*, (2012)[20]	Retrospective	395	62,5	pRCC (Type 1/2)	N/A	Fat invasion: 8%. Sarcomatoid differentiation: 1%.	Tumor size, nuclear grading and lymphovascular invasion were found to affect pRCC prognosis.
Zhu *et al.*, 2013[32]	Retrospective	20	52	cdRCC	3,6	Lower enhancement compared to normal renal cortex	Predominantly medullary, poorly defined and solid, often with cystic or necrotic components, hyperdensity to renal cortex
Hu *et al.*, 2014[33]	Retrospective	6	46	cdRCC	5,3	Weak and heterogeneous enhancement	Predominantly located in the medulla, showed weak and heterogeneous enhancement, frequent infiltrative growth, complex cystic features
Ren *et al.*, 2015[10]	Retrospective	46	58	ccRCC/ONC	ONC: 3,6 ccRCC: 4,3	ONC: Prolonged enhancement. ccRCC: Early washout, higher microvascular density.	ONC: Lower density in corticomedullary phase, higher lesion-to-cortex ratio in nephrographic phase (prolonged enhancement). ccRCC: Higher density in corticomedullary phase
He *et al.*, 2015[7]	Retrospective	17	33,8	Xp11.2 RCC	5,6	Hypervascular in corticomedullary phase, early washout in later phases	Hypervascular, bright contrast in corticomedullary phase, with cystic, heterogeneous areas; potential distinguishing CT features.
Xie *et al.* 2016[8]	Retrospective	82	53	ccRCC/lipid poor AML	4,6	High vascularity	Wash-in and washout on CT can differentiate ccRCC from lipid-poor AML.

(*Contd...*)

Table 1: (*Continued*).

Study	Study design	Number of patients	Mean age (years)	Tumor type	Tumor size (cm)	Vascularity	Main finding
Zhu *et al*., 2017[12]	Retrospective	52	N/A	ccRCC/ONC	N/A	High vascularity, homogeneous contrast pattern	LKR and △LKR from CT phases effectively differentiate ccRCC, chRCC, and ONC with significant sensitivity and specificity
Gentili 2020 [13]	Retrospective	76	63,9	ccRCC, ONC, chRCC, pRCC, mcRCC, AML	2,8	ONC: Isodense ccRCC: Hypodense	RO showed isodense L/C (≥0.9, 80% accuracy) and lower ALAD, with early washout, while RCC was hypodense with prolonged enhancement.
Liang 2021 [36]	Retrospective	125	53.6	ccRCC/pRCC/ chRCC	1,4–11 cm	Moderate vascularity with contrast uptake	CEUS+CECT differentiates RCC subtypes.
Wang *et al*., 2021[9]	Retrospective	105	54,6/51	ccRCC/AML	2,8/2,7	ccRCC shows high vascularity	RER_CMP+SHR_ CMP in CMP phase offers best accuracy
Murugan *et al*., (2022)[16]	Retrospective	199	65	ppRCC (Type 1/2)	3,5	N/A	Type 1 shows good survival; poor prognosis linked to LVI, high mitotic activity, tumor >7 cm, pT3 stage, and sarcomatoid features. Type 1 and 2 share 78% genetic overlap.
Qu *et al*., 2023[37]	Retrospective	81	60	ONC/ccRCC	4,8	Moderate vascularity with mixed enhancement	Peripheral vascularity: L/C ratio oncocytoma ≤1.0, ccRCC>1.0.

RCC: Renal cell carcinoma, CT: Computed tomography, ccRCC:Clear cell RCC, pRCC: Papillary RCC, chRCC: Chromophobe RCC, cdRCC: Collecting duct RCC, mcRCC: Multiloculated cystic RCC, ONC: Oncocytoma, AML: Angiomyolipoma, ALAD: Aorta-lesion-attenuation-difference, N/A: Not applicable, LKR: Lesion-kidney-ration, L/C: Ratio of lesion to cortex, CEUS: Contrast-Enhanced Ultrasound, CECT: Contrast-Enhanced Computed Tomography, RER-CMP: Relative enhancement ratio of corticomedullary phase, SHR: Standardized heterogeneous ratio of corticomedullary phase, LVI: Lenfovascular invasion

renal parenchyma on T1WI and hyperintense on T2WI. These characteristic signal features are important in distinguishing it from other types.[41,42] Necrosis, hemorrhage, and cysts may create variable signals. Necrotic areas are typically observed with high signal on T2WI but not stained on contrast-enhanced series. In dynamic contrast-enhanced MRI, intense contrast enhancement is observed in the corticomedullary phase, while a rapid wash-out is noted in the nephrogenic phase.[43] In addition, a hypointense rim or pseudocapsule formed by tumor growth and compression of adjacent renal parenchyma can be observed on both T1WI and T2WI [Figure 5].

The high vascularity of this type can be clearly assessed with MRI. In particular, ccRCC tumors show contrast enhancement patterns due to their vascular structure. This allows us to better understand the extent of the tumor's blood supply and its relationship with surrounding tissues. The MRI features of ccRCC play a critical role not only in the diagnostic process but also in determining the tumor's prognosis and optimizing the treatment plan.[14]

Beek *et al*. reported that MiT-RCC is characterized by well-defined pseudocapsules and lobulated morphology.[44]

Table 2: MRI characteristics and main findings of renal cell carcinoma (RCC) subtypes across studies.

Study	Study Design	Sample Size	Mean age	Imaging Method	RCC Type	T1 Characteristics	T2 Characteristics	Diffusion Restriction	Enhancement Pattern	Main Findings
Oliva *et al* 2009[41]	Retrospective	45	64	1,5 Tesla MRI	pRCC, ccRCC	No T1 signal intensity ratio differencepRCC vs ccRCC	pRCC: T2 hypointense ccRCC: T2 hyperintense	N/A	N/A	T2 imaging aids RCC differentiation pRCC (T2 hypointense), ccRCC (T2 hyperintense)
Rosenkrantz 2010[55]	Retrospective	41	67	1,5 Tesla MRI	ONC, chRCC	Hypointense	Heterogeneous	lipid noted in some chRCC.	Peripheral, well-circumscribed, no fat/vein invasion, segmental enhancement inversion in 13.3%-42.9%.	Central Scar: 50%-60.7% in ONC, 33.3%-40% in chRCC.
Hindman 2012[61]	Retrospective	23	56	CT/MRI	mcRCC	N/A	N/A	N/A	N/A	McRCC lesions behaved benignly, with no metastasis or recurrence.
Hindman 2012[65]	Retrospective	108	59 (ccRCC) 54(AML)	MRI	ccRCC, AML	Signal loss on opposed-phase imaging showed no significant difference AML and ccRCC	AML: Low SI relative to cortex strongly associated; ccRCC: High SI more frequent.	N/A	Necrosis and cystic degeneration were significantly associated with ccRCC	Opposed-phase imaging lacked reliability, but small size and low T2 SI strongly predicted AML.
Gupta 2012[26]	Clinicopathologic analysis	52	55/22	Various	cdRCC/mRCC	Hypo to isointense	heterogeneous hyperintense	Heterogeneity and restricted diffusion	cdRCC: Heterogeneous mRCC: Rapid, high vascularity	cdRCC: Aggressive, metastatic, desmoplastic stroma, infiltrative margins.mRCC: Highly aggressive, advanced stages, linked to sickle cell anemia.
Zhu 2013[32]	Retrospective	20	52	CT, mpMRI	cdRCC	Isointense	Iso- or hypointense	N/A	lower enhancement	Medullary; poorly defined, often solid with cystic/necrotic changes, may include calcifications, show higher radiodensity on CT, lower enhancement and isointensity on T1/T2 MRI.
Cornelis 2014[45]	Retrospective	90	64,1	mpMRI	ccRCC/pRCC/ chRCC/ONC/ AML	pRCC: Slow and low enhancement. ONC: Early and strong enhancement.	pRCC: Low T2WI chRCC: Intermediate T2WI ONC: T2WI signal is similar to parenchyma.	pRCC: Low ADC ratio (ADCr <54.2). ccRCC: Moderate ADC ratio. ONC: Higher ADC values.	pRCC: Low WiI1 (<30.9). ONC: High WiI2 (>257). chRCC: Delayed WoI2 (> -8.8).	pRCC: Low T2WI signal, low ADC. ONC: High wash-in, low wash-out. Minimal-fat AMLs: High T2WI signal in non-fat saturated sequances.
Murray 2016[6]	Retrospective	64	62,2/57,3	mpMRI	pRCC/AML	Chemical shift T1WI MRI distinguishes pRCC	T2WI alone can't differentiate pRCC and AML	N/A	N/A	Chemical shift MRI aids pRCC distinction but lacks sufficient sensitivity alone.
Jeong 2016[71]	Retrospective	152	N/A	CT/MRI	ccRCC, pRCC, chRCC	Similar for AML (0.97) and RCC (0.89)	Lower in AML (0.75) compared to RCC (1.21)	N/A	N/A	Fat-invisible AML is best differentiated from RCC by tumor-to-cortex ratios on T2WI MRI and unenhanced CT, while chemical-shift MRI shows poor accuracy.
Canvasser 2017[48]	Retrospective	110	57	mpMRI	ccRCC/pRCC/ chRCC/benign	ccRCC: Heterogeneous, microscopic fat.	Mostly high signal.	ccRCC: Intense contrast uptake in cortical regions.	ccRCC: Cortical contrast uptake.	ccRCC: 78% sensitivity, 80% specificity (ccLS 4–5); ccLS 1–2 indicates benign/ non-ccRCC.
Zhang 2017[14]	Prospective	36	58	mpMRI	ccRCC/pRCC/ chRCC/AML	ccRCC: Iso- to hyperintense; pRCC: Hypointense	ccRCC: Hyperintense; pRCC: Hypointense	ccRCC: Variable; pRCC: Minimal	ccRCC: Heterogeneous with high Ktrans and Kep; pRCC: Lower Ktrans and Kep	ASL correlates with DCE; ccRCC: heterogeneous, pRCC: low perfusion
Park 2017[69]	Retrospective	56	54,4(AML) 55,7(RCC)	mpMRI	AML/RCC	No intensity difference AML vs RCC	AML: Predominantly low T2WI intensity	RCC had lower ADC	N/A	ADC predicted RCC vs. AML, with higher accuracy when combined with male sex; minimal-fat AMLs had higher ADC, while T2WI metrics lacked differentiation.
Kay 2018[42]	Retrospective	103	56,7	mpMRI	ccRCC/pRCC/ chRCC/ONC/ AML	Signal intensity in the corticomedullary phase.	ccRCC: High T2 signal; pRCC and benign lesions: Low T2 signal.	N/A	ccRCC: High enhancement; pRCC: Low enhancement; ONC: Segmental enhancement inversion.	Diagnosis accuracy: 81% for ccRCC, 91% for pRcc.
Vendrami *et al* 2018[52]	Retrospective	47	56/60	1,5-3 Tesla mpMRI	pRCC Type1/2	Type1: 54% iso, 23% hypo, 23% hyperintense Type 2: 56% iso, 31% hypo, 13% hyperintense	Type 1: Homogeneous (36%); Heterogeneous (64%) – Type 2: Homogeneous (12%); Heterogeneous (88%)	Type 2 tumors had lower mean ADCs	Type 1: Predominantly homogeneous (65%) Type 2: Predominantly heterogeneous (75%)	Type 2 pRCC shows more heterogeneity, necrosis, and benefits from texture analysis for differentiation.
Johnson 2019[47]	Retrospective	57	61.7	mpMRI (ccLS (Clear Cell Likelihood Score))	ccRCC/pRCC/ chRCC/ONC/ benign	High intravoxel fat signal	Heterogeneous signal in ccRCC, low signal in pRCC	Significant diffusion restriction in ccRCC	Heterogeneous enhancement in ccRCC; homogeneous low enhancement in pRCC.	ccLS 4–5 scored ccRCC at 84% accuracy, ccLS 1–2 scored non-ccRCC at 100%.
Zhu 2021[58]	Retrospective	33	52,1	CT/MRI	mcRCC, cdRCC	Hypointense	mcRCC: Hyperintense; cdRCC: Hypointense	N/A	mcRCC: Thickened enhancing internal septations and mural soft-tissue nodules	mcRCC better-defined boundaries, exogenous growth, and excellent survival, cdRCC infiltrative growth, renal pelvis/ureter involvement, and poor prognosis with high metastasis and mortality.
Steinberg 2021[46]	Retrospective	434	60	mpMRI	ccRCC/pRCC/ chRCC	Assessed per ccLS using intensity patterns	Assessed per ccLS using intensity patterns	B800 diffusion-weighted images.	Heterogeneous, moderate	ccLS1–2: mostly benign; ccLS5: 93% ccRCC
De Silva 2022[62]	Retrospective	66	N/A	3 Tesla MRI	ccRCC/ pRCC/ chRCC/ONC/ AML	Isointense	Hypointense	Moderate restriction	Homogeneous, mild	ONCs the highest ADC (max), pRCC the lowest ADC, ccRCC has higher ADC than pRCC and chRCC
Dunn 2022[63]	Retrospective	102	56.9	1,5 Tesla mpMRI	ccRCC/pRCC/ chRCC/ONC/ AML	ccRCC: Higher signal intensity	ccRCC: Typically T2WI hyperintense	N/A	ccRCC: >75% enhancement; ADER aids subtype differentiation	ccLS: 85% sensitivity, 82% specificity, 83% accuracy; ccLS ≥4 strongly predicts ccRCC
Beek 2023[44]	Retrospective	6	12	1,5 Tesla MRI	MiT-RCC: 2 patients (33%); ccRCC: 2 patients (33%); Other types: 2 patients.	Mostly isointense.	Mostly hypointense	Median ADC: 0.70–1.20 × 10^{-3} mm^2/s; lower in MiT-RCC.	homogeneous strong enhancement	MiT-RCC: T2-hypointense, well-defined pseudocapsules (4/6), median volume 393 cm^3, lobulated shape (4/6).
Wang 2024[56]	Retrospective	105	62	mpMRI	ccRCC, pRCC, chRCC, cdRCC mRCC	Intensity variations, pseudocapsules, and necrosis.	T2WI hyperintense signals. Less hypointense signals in sarcomatoid components.	Lower ADC values indicate higher cellular density and aggressiveness.	Lower TCEI in adverse pathology.	Male gender, high RENAL score, necrosis, irregular margins, and low ADC predict adverse pathology.

ccRCC: Clear cell renal cell cancer, pRCC: Papillary renal cell cancer, chRCC: Chromofobe cell renal cell cancer, mRCC: Medullary RCC, cdRCC: Collecting duct RCC, mcRCC: Multiloculated cystic RCC, AML: Angiomyolipoma, ONC: Oncocytoma

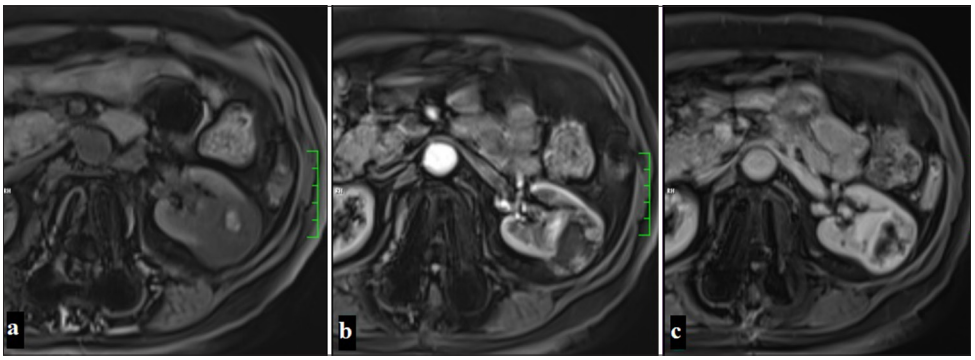

Figure 5: A 60-year-old woman with a lesion observed as hypointense compared to the renal parenchyma in precontrast fat-suppressed T1-weighted imaging, containing a hyperintense area suggestive of focal hemorrhage. The mass shows contrast enhancement except for the central cystic areas in the corticomedullary phase and nephrogenic phase on dynamic MR examination, displayed sequentially in the images (Clear cell renal cell carcinoma).

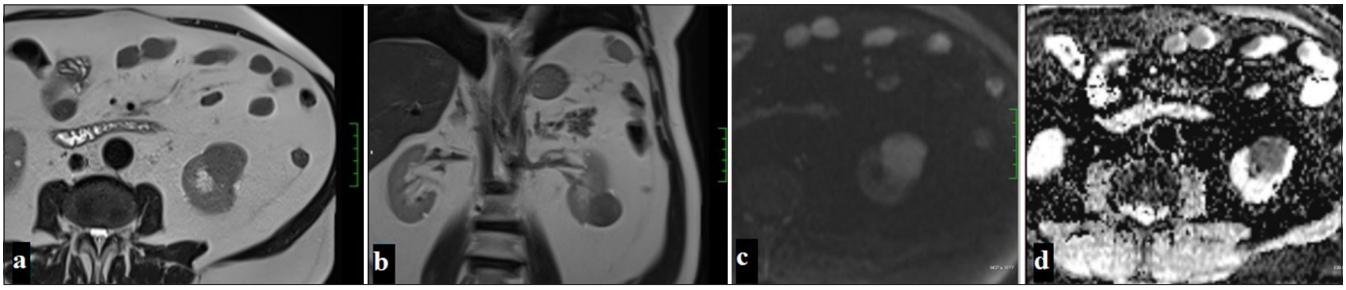

Figure 6: A 54-year-old man with a lesion observed as hypointense in T2-weighted imaging on axial (a) and coronal (b) planes on MRI, hyperintense on DWI (c), and showing diffusion restriction suggestive of malignancy on ADC (d) (Papillary renal cell carcinoma).

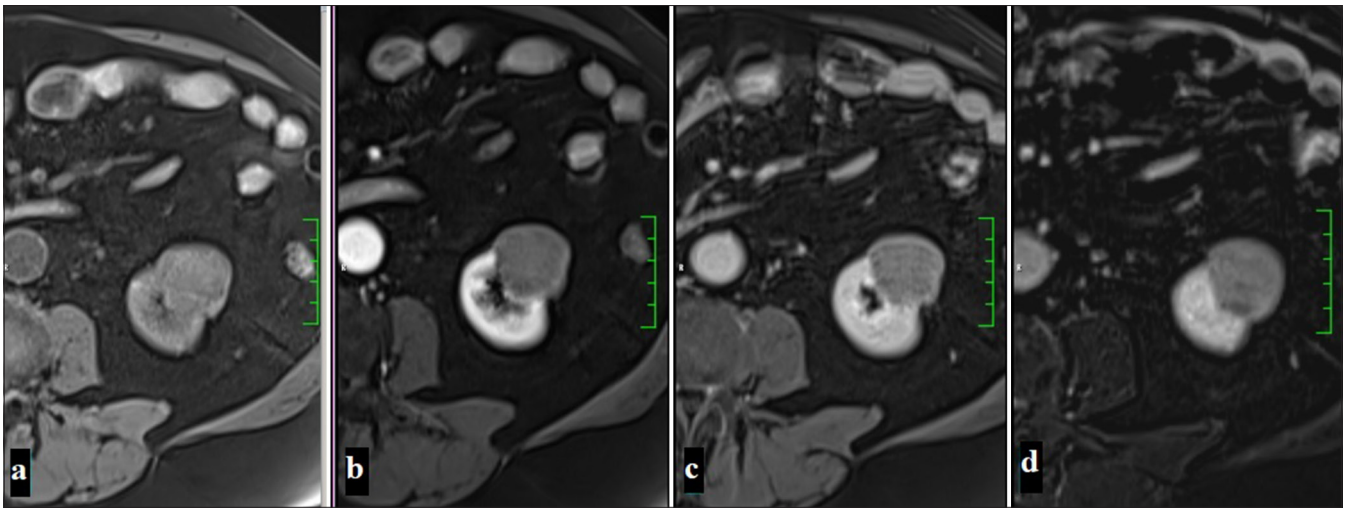

Figure 7: A 54-year-old man with a lesion observed as hypointense in precontrast fat-suppressed T1-weighted imaging (a), showing no significant contrast enhancement in the corticomedullary phase (b) and nephrogenic phase (c), with the subtraction image (d) confirming the absence of contrast enhancement (Papillary renal cell carcinoma).

MRI-based apparent diffusion coefficient (ADC) and contrast pattern analyses have been reported to be important in distinguishing RCC subtypes.[45] It has also been stated that ccRCC and its other subtypes can be accurately classified using the clear cell likelihood score (ccLS) system.[46,47] It has been reported that ccRCC shows high vascularity and cortical

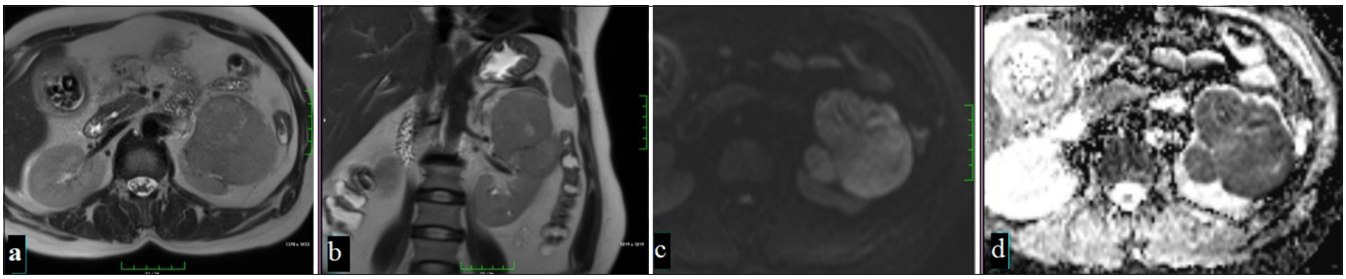

Figure 8: A 53-year-old woman with a mass that is iso-hypointense compared to the renal parenchyma in T2-weighted imaging on axial (a) and coronal (b) planes on MRI, with focal hyperintense areas noted sporadically. The mass is observed to be hyperintense on DWI (c) and shows diffusion restriction suggestive of malignancy on ADC (d) (Chromofobe renal cell carcinoma).

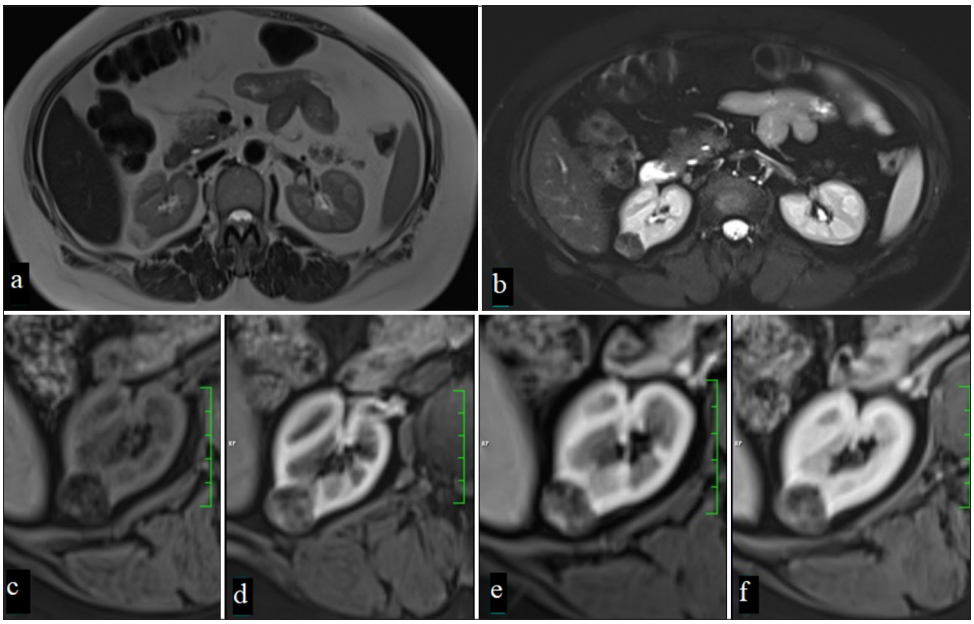

Figure 9: A 67-year-old man with a mass lesion in the right kidney, which appears hyperintense on T2-weighted imaging (a) and shows significant signal loss on fat-suppressed T2-weighted imaging (b) due to macroscopic fat content. In dynamic MRI, the lesion, heterogeneously hypointense compared to the renal parenchyma on precontrast fat-suppressed T1-weighted imaging (c), shows moderate contrast enhancement in the corticomedullary phase (d), nephrogenic phase (e), and (f) late phases (Angiomyolipoma).

contrast enhancement, and the ccLS 4–5 score is effective in identifying ccRCC with 78% sensitivity and 80% specificity.[48]

pRCC

It often tends to grow slowly and presents as well-circumscribed fibrous-encapsulated solid masses. It is usually recognized by hypointense appearance and low contrast enhancement on T2WI on MRI [Figures 6 and 7].[49] Due to its hypovascular characteristics, it shows minimal contrast enhancement in the corticomedullary phase, while it is hypointense compared to the renal parenchyma in the nephrogenic phase. There are studies indicating that the most effective examination in differentiating from ccRCC is the corticomedullary phase.[50] As the lesion size increases, heterogeneity secondary to necrosis, hemorrhage, and calcifications may be observed. It may show also sarcomatous differentiation at a rate of 5%. Type 2 pRCC has been determined to have higher invasiveness than type 1 and to have a more heterogeneous appearance on CT. Similarly, type 2 tumors have been seen to have more frequent infiltrative edges and calcifications on MRI.[51] In addition, the presence of intratumoral hemorrhage on MRI of pRCC stands out as an important feature that can distinguish such tumors from fat-poor angiomyolipomas (AMLs).[6] It has been shown that using quantitative tissue analysis on MRI can differentiate between type 1 and type 2 pRCC, and these analyses can improve model accuracy.[52]

chRCC

This tumor, which is most commonly seen in the 6th decade and has a similar distribution between men and women, is the 3rd most common type of RCC. This tumor, which usually shows a solid growth pattern, is cytogenetically associated with multiple monosomies (1 and 2) and hypodiploidy.[53] It has the best prognosis among RCC types, with a 5-year surveillance of around 78–92%.[24] Often shows high signal intensity on T2A and low homogeneous enhancement after contrast injection.[54] The enhancement patterns of chRCCs show intermediate signal changes compared with other RCC subtypes. For example, the signal intensity change of chRCCs in the corticomedullary phase is lower than that of ccRCC but higher than that of pRCC. ChRCCs show intermediate enhancement in the arterial and venous phases and washout in the late phase [Figure 8].[50]

ChRCC and ONCs may present similar imaging findings due to their similar histological and ontogeny features. ONCs originate from intercalated cells in the collecting ducts and may show central scarring and wheel-like contrast enhancement like chRCC.[55] Among hypovascular tumors, chRCC, which comes after pRCC, can reach large sizes but shows relatively homogeneous contrast enhancement compared to pRCC.

mRCC

This aggressive tumor originates from the medullary collecting ducts and occurs at a young age. It has low signal on T1WI and T2WI in MRI and has invasive features. Heterogeneous contrast enhancement is noted in IV contrast-enhanced MRI.[56] MRCC is often located in the medulla region of the kidney and is observed as a heterogeneous mass with ill-defined borders. The tumor can usually reach large sizes and is often necrotic. MRCC usually has an aggressive course and tends to spread to surrounding tissues, especially caliectasis and retroperitoneal lymph node enlargement. These distinctive features identified on MRI are important in supporting the diagnosis of mRCC, especially in young patients with sickle cell anemia.[57]

Studies have reported that while cdRCC and mcRCC have aggressive biological behaviors and tendencies toward widespread metastasis, mRCC has a better prognosis.[26,58]

cdRCC

This tumor, which is seen in <1%, is a very aggressive subtype of RCC. The average age of onset is 55.[59] On MRI, they appear as masses localized in the medulla, with ill-defined borders, isointense on T1WI, low signal on T2WI, invasive in the medullary region, and showing heterogeneous contrast enhancement.[60] These tumors often appear as heterogeneous complex masses consisting of solid or solid-cystic components.[32] The enhancement patterns are different from other renal tumors. cdRCC shows low contrast enhancement compared to the cortex and medulla; limited enhancement in the corticomedullary phase and no significant washout in the late phases. This weak and heterogeneous enhancement stands out as an important distinguishing feature in diagnosis.[33] It often shows infiltrative growth and tends to spread to the renal pelvis. Invasion of these tumors into surrounding tissues and lymph nodes is common, so the rate of metastasis is high. Perinephric stranding and vascular invasion are often observed on MRI.

mcRCC

This type, encountered as cystic masses separated by septa, may show asymmetric wall thickening. The average age of onset is 51, and the female–male ratio is 1/3. In T2WI on MRI, cystic foci appear hyperintense, while septa appear hypointense. In IV contrast-enhanced MRI, septa become apparent with contrast enhancement.[58] It usually presents as a multi-chambered cystic mass with well-defined, thin septa. In addition, in some cases, small nodular structures or calcifications may be seen on the septa.[61]

De Silva *et al*. and Dunn *et al.* emphasized that ADC values and enhancement patterns present significant differences among RCC subtypes.[62,63] Wang *et al*. showed that low ADC values were associated with increased cellular density and aggressive pathologies.[56] These studies provide important data to more clearly distinguish the imaging findings of different RCC subtypes.

AML and RCC distinction

AML is the most common benign kidney tumor and consists of various dysmorphic vascular structures, smooth muscle cells, and mature fat tissue. The vast majority of this tumor is sporadic and is associated with tuberous sclerosis complex and lymphangioleiomatosis at a rate of 20%.[64] As the tumor size increases, it creates a risk of bleeding due to dilatation and pseudoaneurysm formation in the vascular structures it contains.

CT imaging findings provide decisive features in distinguishing AML from RCC. Classic AMLs can be easily distinguished due to the macroscopic fat they contain, but fat-poor AMLs (<25% fat component) and some types of RCC can be difficult to distinguish by imaging. In AML, the T2A signal increases as the fat content increases, while the decrease in the fat content creates a lower signal [Figure 9].[65] Fat-poor AMLs usually show homogeneous and prolonged enhancement, which is an important distinguishing feature compared to RCC. In studies using CT, 79% of AMLs showed homogeneous enhancement and 58% showed prolonged enhancement; this was found to be much lower in RCC cases.[66] CT histogram analysis is also an effective technique

to distinguish fat-poor AMLs from RCC; densityless than -10 HU is more common in AMLs than in RCC, supporting the diagnosis of AML.[67] In addition, scoring systems developed using multidetector CT help to eliminate the confusion created by different subtypes of RCC and achieve high accuracy in distinguishing AMLs from RCC. In this system, the combination of parameters such as long-short diameter ratio, enhancement characteristics, and homogeneous enhancement increases diagnostic accuracy.[68]

In fat-poor AMLs, the ADC values in DWI are significantly higher than in RCC. This situation stands out as an important criterion in distinguishing AMLs from RCCs, especially in small-sized tumors. Studies have shown that the ADC values of RCCs are lower than AMLs and the accuracy rate of this distinction is quite high.[69]

CSI can also be effective in distinguishing AML and RCC. Studies using chemical shift signal intensity index (CS-SII) values have shown that CS-SII values of fat-poor AMLs are higher than those of RCC. This technique is particularly useful in defining RCC subtypes. CS-SII values support the characterization of AML as well as pRCC and chRCC subtypes.[70]

Fat-poor AMLs with low signal intensity on T2WI MRIs can also be distinguished from RCC. This low signal intensity is a distinguishing feature, especially when combined with ADC, and supports the correct diagnosis in small renal masses. However, this feature does not differ from some other RCC subtypes, and biopsy may be required for definitive differentiation.[71] Hindman N *et al*. emphasized the importance of T2 signal intensity and cystic degeneration in distinguishing AML with minimal fat and ccRCC[65] [Table 2].

CONCLUSİON

The different histopathological subtypes of RCC can be better understood by characterizing them with advanced imaging modalities such as CT and MRI. Examining the imaging features of these subtypes plays a critical role in the diagnosis and treatment process, providing important insights into each subtype's unique clinical course and prognosis. Therefore, detailing the imaging findings of RCC contributes to the identification of more targeted treatment approaches and plays a key role in improving patient outcomes.

Ethical approval: The Institutional Review Board approval is not required.
Declaration of patient consent: Patient consent is not required as this is a review article and does not involve any patient data or identifiable information.
Financial support and sponsorship: Nil.
Use of artificial intelligence (AI)-assisted technology for manuscript preparation: The authors confirm that there was no use of artificial intelligence (AI)-assisted technology for assisting in the writing or editing of the manuscript and no images were manipulated using AI.

REFERENCES

1. Reuter VE, Humphrey PA, Ulbright TM, Moch H. WHO classification of tumours of the urinary system and male genital organs. France: IARC; 2016. p. 189-226.
2. Rini BI, Campbell SC, Escudier B. Renal cell carcinoma. Lancet 2009;373:1119-32.
3. Ljungberg B, Albiges L, Abu-Ghanem Y, Bedke J, Capitanio U, Dabestani S, *et al*. European Association of Urology guidelines on renal cell carcinoma: The 2022 update. Eur Urol 2022;82:399-410.
4. Chandrasekar T, Klaassen Z, Goldberg H, Kulkarni GS, Hamilton RJ, Fleshner NE. Metastatic renal cell carcinoma: Patterns and predictors of metastases-A contemporary population-based series. Urol Oncol 2017;35:661.e7-14.
5. Sun M, Thuret R, Abdollah F, Lughezzani G, Schmitges J, Tian Z, *et al*. Age-adjusted incidence, mortality, and survival rates of stage-specific renal cell carcinoma in North America: A trend analysis. Eur Urol 2011;59:135-41.
6. Murray CA, Quon M, McInnes MD, van der Pol CB, Hakim SW, Flood TA, *et al*. Evaluation of T1-weighted MRI to detect intratumoral hemorrhage within papillary renal cell carcinoma as a feature differentiating from angiomyolipoma without visible fat. AJR Am J Roentgenol 2016;207:585-91.
7. He J, Gan W, Liu S, Zhou K, Zhang G, Guo H, *et al*. Dynamic computed tomographic features of adult renal cell carcinoma associated with Xp11. 2 translocation/TFE3 gene fusions: Comparison with clear cell renal cell carcinoma. J Comput Assist Tomogr 2015;39:730-6.
8. Xie P, Yang Z, Yuan Z. Lipid-poor renal angiomyolipoma: Differentiation from clear cell renal cell carcinoma using wash-in and washout characteristics on contrast-enhanced computed tomography. Oncol Lett 2016;11:2327-31.
9. Wang X, Song G, Jiang H. Differentiation of renal angiomyolipoma without visible fat from small clear cell renal cell carcinoma by using specific region of interest on contrast-enhanced CT: A new combination of quantitative tools. Cancer Imaging 2021;21:47.
10. Ren A, Cai F, Shang YN, Ma ES, Huang ZG, Wang W, *et al*. Differentiation of renal oncocytoma and renal clear cell carcinoma using relative CT enhancement ratio. Chin Med J (Engl) 2015;128:175-9.
11. Shen J, Zou Y. Diagnostic value of contrast-enhanced CT in clear cell renal cell carcinoma: A systematic review and meta-analysis. BMC Urol 2024;24:189.
12. Zhu G, Li Z, Liang J, Zeng Z, Tao J. Comparison of multi-slice spiral CT features of chromophobe renal cell carcinoma, renal oncocytoma and clear-cell renal cell carcinoma. Chin J Med Imaging 2017;12:136-140, 145.
13. Gentili F, Bronico I, Maestroni U, Ziglioli F, Silini EM, Buti S, *et al*. Small renal masses (≤4 cm): Differentiation of oncocytoma from renal clear cell carcinoma using ratio of lesion to cortex attenuation and aorta-lesion attenuation difference (ALAD) on contrast-enhanced CT. Radiol Med 2020;125:1280-7.

14. Zhang Y, Kapur P, Yuan Q, Xi Y, Carvo I, Signoretti S, *et al.* Tumor vascularity in renal masses: Correlation of arterial spin-labeled and dynamic contrast-enhanced magnetic resonance imaging assessments. Clin Genitourin Cancer 2016;14:e25-36.
15. Zhang J, Lefkowitz RA, Ishill NM, Wang L, Moskowitz CS, Russo P, *et al.* Solid renal cortical tumors: Differentiation with CT. Radiology 2007;244:494-504.
16. Murugan P, Jia L, Dinatale RG, Assel M, Benfante N, Al-Ahmadie HA, *et al.* Papillary renal cell carcinoma: A single institutional study of 199 cases addressing classification, clinicopathologic and molecular features, and treatment outcome. Mod Pathol 2022;35:825-35.
17. Marston Linehan W, Spellman PT, Ricketts CJ, Creighton CJ, Fei SS, Davis C, *et al.* Comprehensive molecular characterization of papillary renal-cell carcinoma. N Engl J Med 2016;374:135-45.
18. Delahunt B, Eble JN. Papillary renal cell carcinoma: A clinicopathologic and immunohistochemical study of 105 tumors. Mod Pathol 1997;10:537-44.
19. Klatte T, Pantuck AJ, Said JW, Seligson DB, Rao NP, LaRochelle JC, *et al.* Cytogenetic and molecular tumor profiling for type 1 and type 2 papillary renal cell carcinoma. Clin Cancer Res 2009;15:1162-9.
20. Sukov WR, Lohse CM, Leibovich BC, Thompson RH, Cheville JC. Clinical and pathological features associated with prognosis in patients with papillary renal cell carcinoma. J Urol 2012;187:54-9.
21. Antonelli A, Tardanico R, Balzarini P, Arrighi N, Perucchini L, Zanotelli T, *et al.* Cytogenetic features, clinical significance and prognostic impact of type 1 and type 2 papillary renal cell carcinoma. Cancer Genet Cytogenet 2010;199:128-33.
22. Morshid A, Duran ES, Choi WJ, Duran C. A Concise review of the multimodality imaging features of renal cell carcinoma. Cureus 2021;13:e13231.
23. Amin MB, Amin MB, Tamboli P, Javidan J, Stricker H, de-Peralta Venturina M, *et al.* Prognostic impact of histologic subtyping of adult renal epithelial neoplasms: An experience of 405 cases. Am J Surg Pathol 2002;26:281-91.
24. Cheville JC, Lohse CM, Zincke H, Weaver AL, Blute ML. Comparisons of outcome and prognostic features among histologic subtypes of renal cell carcinoma. Am J Surg Pathol 2003;27:612-24.
25. Przybycin CG, Cronin AM, Darvishian F, Gopalan A, Al-Ahmadie HA, Fine SW, *et al.* Chromophobe renal cell carcinoma: A clinicopathologic study of 203 tumors in 200 patients with primary resection at a single institution. Am J Surg Pathol 2011;35:962-70.
26. Gupta R, Billis A, Shah RB, Moch H, Osunkoya AO, Jochum W, *et al.* Carcinoma of the collecting ducts of Bellini and renal medullary carcinoma: Clinicopathologic analysis of 52 cases of rare aggressive subtypes of renal cell carcinoma with a focus on their interrelationship. Am J Surg Pathol 2012;36:1265-78.
27. Greco F, Faiella E, Santucci D, Mallio CA, Nezzo M, Quattrocchi CC, *et al.* Imaging of renal medullary carcinoma. J Kidney Cancer VHL 2017;4:1-7.
28. Lebenthal JM, Kontoyiannis PD, Hahn AW, Lim ZD, Rao P, Cheng JP, *et al.* Clinical characteristics, management, and outcomes of patients with renal medullary carcinoma: A single-center retrospective analysis of 135 patients. Eur Urol Oncol 2024;S2588-9311(24)00175-5.
29. Swartz MA, Karth J, Schneider DT, Rodriguez R, Beckwith JB, Perlman EJ. Renal medullary carcinoma: Clinical, pathologic, immunohistochemical, and genetic analysis with pathogenetic implications. Urology 2002;60:1083-9.
30. Muglia VF, Prando A. Renal cell carcinoma: Histological classification and correlation with imaging findings. Radiol Bras 2015;48:166-74.
31. Karakiewicz PI, Trinh QD, Rioux-Leclercq N, de la Taille A, Novara G, Tostain J, *et al.* Collecting duct renal cell carcinoma: A matched analysis of 41 cases. Eur Urol 2007;52:1140-6.
32. Zhu Q, Wu J, Wang Z, Zhu W, Chen W, Wang S. The MSCT and MRI findings of collecting duct carcinoma. Clin Radiol 2013;68:1002-7.
33. Hu Y, Lu GM, Li K, Zhang LJ, Zhu H. Collecting duct carcinoma of the kidney: Imaging observations of a rare tumor. Oncol Lett 2014;7:519-24.
34. Gong K, Zhang N, He Z, Zhou L, Lin G, Na Y. Multilocular cystic renal cell carcinoma: An experience of clinical management for 31 cases. J Cancer Res Clin Oncol 2008;134:433-7.
35. Suzigan S, López-Beltrán A, Montironi R, Drut R, Romero A, Hayashi T, *et al.* Multilocular cystic renal cell carcinoma: A report of 45 cases of a kidney tumor of low malignant potential. Am J Clin Pathol 2006;125:217-22.
36. Liang RX, Wang H, Zhang HP, Ye Q, Zhang Y, Zheng MJ, *et al.* The value of real-time contrast-enhanced ultrasound combined with CT enhancement in the differentiation of subtypes of renal cell carcinoma. Urol Oncol 2021;39:837.e19-28.
37. Qu JY, Jiang H, Song XH, Wu JK, Ma H. Four-phase computed tomography helps differentiation of renal oncocytoma with central hypodense areas from clear cell renal cell carcinoma. Diagn Interv Radiol 2023;29:205-11.
38. Kang SK, Chandarana H. Contemporary imaging of the renal mass. Urol Clin North Am 2012;39:161-70, vi.
39. Pedrosa I, Alsop DC, Rofsky NM. Magnetic resonance imaging as a biomarker in renal cell carcinoma. Cancer 2009;115:2334-45.
40. Polascik TJ, Bostwick DG, Cairns P. Molecular genetics and histopathologic features of adult distal nephron tumors. Urology 2002;60:941-6.
41. Oliva MR, Glickman JN, Zou KH, Teo SY, Mortelé KJ, Rocha MS, *et al.* Renal cell carcinoma: T1 and t2 signal intensity characteristics of papillary and clear cell types correlated with pathology. AJR Am J Roentgenol 2009;192:1524-30.
42. Kay FU, Canvasser NE, Xi Y, Pinho DF, Costa DN, Diaz de Leon A, *et al.* Diagnostic performance and interreader agreement of a standardized MR imaging approach in the prediction of small renal mass histology. Radiology 2018;287:543-53.
43. Lopes Vendrami C, Parada Villavicencio C, DeJulio TJ, Chatterjee A, Casalino DD, Horowitz JM, *et al.* Differentiation of solid renal tumors with multiparametric MR imaging. Radiographics 2017;37:2026-42.
44. Beek JN, Krijger RR, Nievelstein RA, Bex A, Klijn AJ, Heuvel-Eibrink MM, *et al.* MRI characteristics of pediatric and young-adult renal cell carcinoma: A single-center retrospective study and literature review. Cancers (Basel) 2023;15:1401.

45. Cornelis F, Tricaud E, Lasserre AS, Petitpierre F, Bernhard JC, Le Bras Y, *et al.* Routinely performed multiparametric magnetic resonance imaging helps to differentiate common subtypes of renal tumours. Eur Radiol 2014;24:1068-80.
46. Steinberg RL, Rasmussen RG, Johnson BA, Ghandour R, De Leon AD, Xi Y, *et al.* Prospective performance of clear cell likelihood scores (ccLS) in renal masses evaluated with multiparametric magnetic resonance imaging. Eur Radiol 2021;31:314-24.
47. Johnson BA, Kim S, Steinberg RL, de Leon AD, Pedrosa I, Cadeddu JA. Diagnostic performance of prospectively assigned clear cell Likelihood scores (ccLS) in small renal masses at multiparametric magnetic resonance imaging. Urol Oncol 2019;37:941-6.
48. Canvasser NE, Kay FU, Xi Y, Pinho DF, Costa D, de Leon AD, *et al.* Diagnostic accuracy of multiparametric magnetic resonance imaging to identify clear cell renal cell carcinoma in cT1a renal masses. J Urol 2017;198:780-6.
49. Patel A. Indeterminate renal lesions: A pragmatic imaging approach. In: European Congress of Radiology (ECR) 2018. Vol. 21; 2016. p. 86.
50. Sun MR, Ngo L, Genega EM, Atkins MB, Finn ME, Rofsky NM, *et al.* Renal cell carcinoma: Dynamic contrast-enhanced MR imaging for differentiation of tumor subtypes--correlation with pathologic findings. Radiology 2009;250:793-802.
51. Egbert ND, Caoili EM, Cohan RH, Davenport MS, Francis IR, Priya Kunju L, *et al.* Differentiation of papillary renal cell carcinoma subtypes on CT and MRI. AJR Am J Roentgenol 2013;201:347-55.
52. Vendrami CL, Velichko YS, Miller FH, Chatterjee A, Villavicencio CP, Yaghmai V, *et al.* Differentiation of papillary renal cell carcinoma subtypes on MRI: Qualitative and texture analysis. AJR Am J Roentgenol 2018;211:1234-45.
53. Eble JN, Sauter G, Epstein JI, Sesterhenn IA, editors. Pathology and genetics of tumours of the urinary system and male genital organs. Switzerland: World Health Organization; 2004. p. 65-7.
54. Ng KL, Rajandram R, Morais C, Yap NY, Samaratunga H, Gobe GC, *et al.* Differentiation of oncocytoma from chromophobe renal cell carcinoma (RCC): Can novel molecular biomarkers help solve an old problem? J Clin Pathol 2014;67:97-104.
55. Rosenkrantz AB, Hindman N, Fitzgerald EF, Niver BE, Melamed J, Babb JS. MRI features of renal oncocytoma and chromophobe renal cell carcinoma. AJR Am J Roentgenol 2010;195:W421-7.
56. Wang K, Guo B, Yao Z, Li G. Clinical T1/2 renal cell carcinoma: Multiparametric dynamic contrast-enhanced MRI features-based model for the prediction of individual adverse pathology. World J Surg Oncol 2024;22:145.
57. Blitman NM, Berkenblit RG, Rozenblit AM, Levin TL. Renal medullary carcinoma: CT and MRI features. AJR Am J Roentgenol 2005;185:268-72.
58. Zhu Q, Ling J, Ye J, Zhu W, Wu J, Chen W. CT and MRI findings of cystic renal cell carcinoma: Comparison with cystic collecting duct carcinoma. Cancer Imaging 2021;21:52.
59. Prasad SR, Humphrey PA, Catena JR, Narra VR, Srigley JR, Cortez AD, *et al.* Common and uncommon histologic subtypes of renal cell carcinoma: Imaging spectrum with pathologic correlation. Radiographics 2006;26:1795-806.
60. Suarez C, Marmolejo D, Valdivia A, Morales-Barrera R, Gonzalez M, Mateo J, *et al.* Update in collecting duct carcinoma: Current aspects of the clinical and molecular characterization of an orphan disease. Front Oncol 2022;12:970199.
61. Hindman NM, Bosniak MA, Rosenkrantz AB, Lee-Felker S, Melamed J. Multilocular cystic renal cell carcinoma: Comparison of imaging and pathologic findings. AJR Am J Roentgenol 2012;198:W20-6.
62. De Silva S, Lockhart KR, Aslan P, Nash P, Hutton A, Malouf D, *et al.* The diagnostic utility of diffusion weighted MRI imaging and ADC ratio to distinguish benign from malignant renal masses: Sorting the kittens from the tigers. BMC Urol 2021;21:67.
63. Dunn M, Linehan V, Clarke SE, Keough V, Nelson R, Costa AF. Diagnostic performance and interreader agreement of the MRI clear cell likelihood score for characterization of cT1a and cT1b solid renal masses: An external validation study. AJR Am J Roentgenol 2022;219:793-803.
64. Jinzaki M, Silverman SG, Akita H, Nagashima Y, Mikami S, Oya M. Renal angiomyolipoma: A radiological classification and update on recent developments in diagnosis and management. Abdom Imaging 2014;39:588-604.
65. Hindman N, Ngo L, Genega EM, Melamed J, Wei J, Braza JM, *et al*. Angiomyolipoma with minimal fat: Can it be differentiated from clear cell renal cell carcinoma by using standard MR techniques? Radiology 2012;265:468-77.
66. Kim JK, Park SY, Shon JH, Cho KS. Angiomyolipoma with minimal fat: Differentiation from renal cell carcinoma at biphasic helical CT. Radiology 2004;230:677-84.
67. Kim JY, Kim JK, Kim N, Cho KS. CT histogram analysis: Differentiation of angiomyolipoma without visible fat from renal cell carcinoma at CT imaging. Radiology 2008;246:472-9.
68. Kim MH, Lee J, Cho G, Cho KS, Kim J, Kim JK. MDCT-based scoring system for differentiating angiomyolipoma with minimal fat from renal cell carcinoma. Acta Radiol 2013;54:1201-9.
69. Park JJ, Kim CK. Small (< 4 cm) renal tumors with predominantly low signal intensity on T2-weighted images: Differentiation of minimal-fat angiomyolipoma from renal cell carcinoma. AJR Am J Roentgenol 2017;208:124-30.
70. Chen LS, Zhu ZQ, Wang ZT, Li J, Liang LF, Jin JY, *et al.* Chemical shift magnetic resonance imaging for distinguishing minimal-fat renal angiomyolipoma from renal cell carcinoma: A meta-analysis. Eur Radiol 2018;28:1854-61.
71. Jeong CJ, Park BK, Park JJ, Kim CK. Unenhanced CT and MRI parameters that can be used to reliably predict fat-invisible angiomyolipoma. AJR Am J Roentgenol 2016;206:340-7.

How to cite this article: Baytok A, Ecer G, Balasar M, Koplay M. Computed tomography and magnetic resonance imaging characteristics of renal cell carcinoma: Differences between subtypes and clinical evaluation. J Clin Imaging Sci. 2025;15:10. doi: 10.25259/JCIS_160_2024